

# Sketching for Sequential Change-Point Detection

Yang Cao, Andrew Thompson, Meng Wang, and Yao Xie

**Abstract**—We study sequential change-point detection procedures using linear sketches of high-dimensional signal vectors, using the generalized likelihood ratio (GLR) statistics. The GLR statistic has the benefit that it allows for unknown post-change mean, which is a better model for the anomaly or novelty detection. We consider both fixed and time-varying projections, derive theoretical approximations to two fundamental performance metrics: the average run length (ARL) and the expected detection delay (EDD); these approximations are shown to be highly accurate by numerical simulations. There is a trade-off in complexity and performance for sketching procedure; we characterize such trade-off and show that the performance loss of using sketching can be bounded. Finally, we demonstrate the good performance of the sketching performance using simulation and real-data examples on solar flare detection and failure detection in power networks.

## I. INTRODUCTION

Online change-point detection from high-dimensional streaming data is a problem arising frequently from applications such as real-time monitoring for sensor networks, computer network anomaly detection and computer vision (e.g. [2], [3]). To reduce data dimensionality, a common approach is *sketching* [4], which performs random projection of the high-dimensional data vectors into lower-dimensional ones.

In this paper, we consider change-point detection using linear sketches of high-dimensional data vectors, and present a new sequential *sketching procedure* based on the generalized likelihood ratio (GLR) statistics. In particular, suppose we may choose an  $M \times N$  matrix  $A$  with  $M \ll N$  to project the original data  $y_t = Ax_t$ ,  $t = 1, 2, \dots$ . Assume the pre-change vector is zero-mean Gaussian distributed, and the post-change vector is Gaussian distributed with an *unknown* mean vector  $\mu$ , with the covariance matrix unchanged. Here we assume the mean vector is unknown since it typically represents an anomaly. The GLR statistic is formed by replacing the unknown  $\mu$  with its maximum likelihood ratio estimator (such approach is commonly used, see, e.g., for genomic copy number variation detection [5]). Then we further generalize to the setting with time-varying projections  $A_t$  of dimension  $M_t \times N$ . Finally, we demonstrate the good performance of our procedures on a real data example of solar flare detection

and a synthetic example of power network failure detection with real-world power network topology.

One interesting aspect of this problem is that to achieve dimensionality reduction; there are typically fewer number of linear projections than the ambient dimension of the data. Thus we are not able to find a unique estimator for the mean. Instead, we pick an arbitrary point from the set of estimators to form the GLR statistic. We show that such a GLR statistic can achieve reasonable performance: the detection performance loss relative to the procedure using full data can be bounded by a small number. In this sense, we find that the task of detecting the presence of a signal from its linear projection is much easier than the corresponding tasks of recovering the signal itself.

Our theoretical contribution is two-fold. First, we obtain analytic expressions for two fundamental performance metrics for the sketching procedures: the average run length (ARL) when there is no change and the expected detection delay (EDD) when there is a change-point, for both fixed and time-varying projections. Our approximations are shown to be highly accurate using simulations. These approximations are quite useful in determining the threshold of the detection procedure to control false-alarms, without having to resort to the onerous numerical simulations.

Second, we characterize a performance-complexity trade-off for the sketching procedure. We examine the EDD ratio between the sketching procedure and a procedure using the original data when the sketching matrix  $A$  is either a random Gaussian matrix or a sparse 0-1 matrix (in particular, an expander graph). We find that the sketching procedure may achieve a performance very similar to that using the original data when the signal-to-noise ratio is sufficiently large, even when the post-change mean vector is not sparse. This result is also verified numerically.

Our notations are standard:  $\chi_k^2$  denotes the Chi-square distribution with degree-of-freedom  $k$ ,  $I_n$  denotes an identity matrix of size  $n$ ;  $X^\dagger$  denotes the pseudoinverse of a matrix  $X$ ;  $[x]_i$  denotes the  $i$ th coordinate of a vector  $x$ ;  $[X]_{ij}$  denotes the  $ij$ th element of a matrix  $X$ ;  $x^\top$  denotes the transpose of a vector or matrix  $x$ .

The rest of the sections are organized as follows. We first review some closely related work. Section II sets up the formulation of the sketching problem for sequential change-point detection. Section III presents the sketching procedures. Section IV and Section V contain the performance analysis of the sketching procedures. Section VI and Section VII demonstrate good performance of our sketching procedures using simulation and real-world examples. Section VIII concludes the paper. All proofs are delegated to the appendix.

Yang Cao (Email: caoyang@gatech.edu) and Yao Xie (Email: yao.xie@isye.gatech.edu) are with the H. Milton Stewart School of Industrial and Systems Engineering, Georgia Institute of Technology, Atlanta, GA, USA. Andrew Thompson (Email: thompson@maths.ox.ac.uk) is with the Mathematical Institute, University of Oxford, Oxford, UK. Meng Wang (Email: wangm7@rpi.edu) is with the Department of Electrical, Computer & Systems Engineering, Rensselaer Polytechnic Institute, Troy, NY, USA. Authors are listed alphabetically. Part of the paper has appeared in our GlobalSIP 2015 paper [1].

### A. Related work

Change-point detection problems are closely related to industrial quality control and multivariate statistical control charts (SPC), where an observed process is assumed initially to be in control and at a change-point becomes out of control. The idea of using random projections for change detection has been explored for SPC in a pioneering work [6] based on  $U^2$  multivariate control chart, the follow-up work [7] for cumulative sum (CUSUM) control chart and the exponential weighting moving average (EWMA) schemes, and in [8], [9] based on the Hotelling statistic. These works provide a complementary perspective from SPC design, while our method takes a different approach and is based on sequential hypothesis testing, treating both the change-point location and the post-change mean vector as unknown parameters. By treating the change-point location as an unknown parameter when deriving the detection statistic, the sequential hypothesis testing approach overcomes the drawback of some SPC methods due to a lack-of-memory, such as the Shewhart chart and the Hotelling chart, since they cannot utilize the information embedded in the entire sequence [10]. Moreover, our sequential GLR statistic may be preferred over the CUSUM procedure in the setting when it is difficult to specify the post-change mean vector. Besides the above distinctions from the SPC methods, other novelty of our methods also include: (1) we developed new theoretical results for the sequential GLR statistic, combining analytical techniques for sequential change-point detection and compressed sensing; (2) we consider the sparse 0-1 and time-varying projections (the sparse 0-1 projection corresponds to sampling the observations and is easily usable in practice); the analysis of these two cases are completely new and not taken from literature; (3) we study the amount of dimensionality reduction can be performed (i.e., the minimum  $M$ ) with little performance loss.

This paper extends on our preliminary work reported in [1]. Moreover, we provide several important extensions: (1) we introduce time-varying sketching projections, which is more widely applicable, and provide theoretical performance analysis; (2) we include more extensive numerical examples to verify the accuracy of our theoretical results analysis; (3) we include new real-data examples to show the good performance of our sketching procedures for solar flare detection and power failure detection.

Our work is related to compressive signal processing [11], where the problem of interest is to estimate or detect (in the fixed-sample setting) a sparse signal using compressive measurements. In [12], an offline test for a non-zero vector buried in Gaussian noise using noise linear measurements is studied; interestingly, a conclusion similar to ours is drawn that the task of detection within this setting is much easier than the tasks of estimation and support recovery. Another related work is [13], which considers a problem of identifying a subset of data streams within a larger set, where the data streams in the subset follow a distribution (representing anomaly) that is different from the original distribution; the problem considered therein is not a sequential change-point

detection problem as the “change-point” happens at the onset ( $t = 1$ ). In [14], the authors also consider an offline setting with one sequence of samples and the goal is to identify  $k$  out of  $n$  samples whose distributions are different from the normal distribution  $f_0$ . They use a “temporal” mixing of the samples over this finite horizon. This is different from our setting, where we project over the signal dimension at each time. In [15], change-point detection using “compressive” measurements of a high-dimensional vector is studied in a Bayesian framework (i.e., Shiryaev’s procedure); theoretical analysis of average detection delay is presented. Other related methods include applying kernel methods [16] and [17] but they focus on offline change-point detection. Finally, using change-point detection for detecting a transient change in power systems has been studied in [18], and the method is tailored to a physical dynamic model of the real-world power system.

Another possible approach is to obtain compressed representations of the data streams by applying principal component analysis (PCA) [19]. The dimensionality reduction by PCA is achieved by projecting the signal along a fixed subspace, which is defined by the eigenspace of the signal associated with the dominant eigenvalues. Our theoretical approximation for ARL and EDD can also be applied in those settings. However, when the dimension of the data is really large, it is hard to implement PCA-base method [20].

## II. FORMULATION

Consider a sequence of observations over a possibly infinite time horizon  $x_1, x_2, \dots, x_t$ ,  $t = 1, 2, \dots$ , where  $x_t \in \mathbb{R}^N$  and  $N$  is the signal dimension. Initially the observations are due to noise. There can be a time  $\kappa$  such that an unknown change-point occurs and it changes the mean of the signal vector. Such a problem can be formulated as the following hypothesis testing problem:

$$\begin{aligned} H_0 : & \quad x_t \sim \mathcal{N}(0, I_N), \quad t = 1, 2, \dots \\ H_1 : & \quad x_t \sim \mathcal{N}(0, I_N), \quad t = 1, 2, \dots, \kappa, \\ & \quad x_t \sim \mathcal{N}(\mu, I_N), \quad t = \kappa + 1, \kappa + 2, \dots \end{aligned} \quad (1)$$

where the *unknown* mean vector is defined as

$$\mu \triangleq [\mu_1, \dots, \mu_N]^T \in \mathbb{R}^N.$$

Our goal is to detect the change-point as soon as possible after it occurs, while subject to the false alarm constraints. Here, we assume the covariance of the data to be an identity matrix, and the change only occurs to the mean.

To reduce data dimensionality, we linearly project each signal  $x_t$  into a lower dimensional space, which we refer to as *sketching*. We aim to develop procedures that can detect a change-point using the low-dimensional *sketches*. In the following, we consider two types of linear sketching: the fixed projection and the time-varying projection.

*Fixed projection.* Choose an  $M \times N$  projection matrix  $A$  with  $M \ll N$  and obtain low dimensional sketches via:

$$y_t \triangleq Ax_t, \quad t = 1, 2, \dots \quad (2)$$

From the earlier model (1), the hypothesis test in terms of the sketches (2) can be reformulated as

$$\begin{aligned} H_0 : y_t &\sim \mathcal{N}(0, AA^\top), \quad t = 1, 2, \dots \\ H_1 : y_t &\sim \mathcal{N}(0, AA^\top), \quad t = 1, 2, \dots, \kappa, \\ &y_t \sim \mathcal{N}(A\mu, AA^\top), \quad t = \kappa + 1, \kappa + 2, \dots \end{aligned} \quad (3)$$

Note that both mean and covariance structures are changed due to projections.

*Time-varying projection.* In certain applications, sketching matrix may be different at each time. In this setting, the projection  $A_t \in \mathbb{R}^{M_t \times N}$ , where the number of sketches  $M_t$  can be time-varying as well. The hypothesis test based on the sketches becomes:

$$\begin{aligned} H_0 : y_t &\sim \mathcal{N}(0, A_t A_t^\top), \quad t = 1, 2, \dots \\ H_1 : y_t &\sim \mathcal{N}(0, A_t A_t^\top), \quad t = 1, 2, \dots, \kappa, \\ &y_t \sim \mathcal{N}(A_t \mu, A_t A_t^\top), \quad t = \kappa + 1, \kappa + 2, \dots \end{aligned} \quad (4)$$

The above models also capture several important cases:

- (i) (Pairwise comparison.) In certain problems such as social network study and computer vision, we are interested in pairwise comparison of variables [21], [22]. This will entail a total of  $N^2$  possible comparison results, and we may select  $M$  out of  $N^2$  such comparisons to reduce complexity. Such pairwise comparison problems can be modeled as structured fixed projections  $A$  with only  $\{0, 1, -1\}$  entries, for instance:

$$A = \begin{bmatrix} 1 & -1 & 0 & \dots & 0 & 0 \\ 1 & 0 & 0 & \dots & -1 & 0 \\ \dots & \dots & \dots & \dots & \dots & \dots \\ 0 & 1 & 0 & \dots & 0 & -1 \end{bmatrix} \in \mathbb{R}^{M \times N}.$$

Note that one may only perform a subset of  $M$  comparisons.

- (ii) (Missing data.) In many scenarios, each time we are only able to observe a subset of entries of the signal, and the location of the entries that we can observe can vary with time [23]. This setting can be captured by letting  $A_t \in \mathbb{R}^{M_t \times N}$  be a submatrix of an identity matrix with rows selected according to  $\Omega_t$ , which is a subset of entries that we observe at time  $t$ .
- (iii) (PCA.) There are also approaches to change-point detection using principal component analysis (PCA) of the data streams (e.g., [19], [24]). The main idea is to extract the several principle components of the data streams, and then form a SPC control chart or a CUSUM procedure with these principle components. Note that this method can be viewed as using a fixed projection  $A$ , with  $A$  being the basis of the signal eigenspace associated with the dominant eigenvalues.

### III. SKETCHING PROCEDURE

#### A. Fixed projection

1) *Derivation of GLR statistic:* We now derive a likelihood ratio based detection procedure for the hypothesis test (3).

Define an average of samples within a window  $[k, t]$

$$\bar{y}_{k,t} = \frac{\sum_{i=k+1}^t y_i}{t-k}. \quad (5)$$

Since the observations are i.i.d. over time, for an assumed value of the change-point  $\kappa = k$ , for the hypothesis test (3), the log-likelihood (log-LR) of observations accumulated up to time  $t > k$  can be shown to be

$$\begin{aligned} \ell(t, k, \mu) &= (t-k)[\bar{y}_{k,t}^\top (AA^\top)^{-1} A\mu - \frac{1}{2} \mu^\top A^\top (AA^\top)^{-1} A\mu]. \end{aligned} \quad (6)$$

Since  $\mu$  is unknown, we replace it with a maximum likelihood estimator for fixed  $k$  and  $t$  in the likelihood ratio (6) to obtain the log generalized likelihood ratio (log-GLR) statistic. Taking the derivative of  $\ell(t, k, \mu)$  in (6) with respect to  $\mu$  and setting it to zero, we obtain an equation that the maximum likelihood estimate  $\mu^*$  of the post-change mean vector needs to satisfy:

$$A^\top (AA^\top)^{-1} A\mu^* = A^\top (AA^\top)^{-1} \bar{y}_{t,k}, \quad (7)$$

or equivalently

$$A^\top [(AA^\top)^{-1} A\mu^* - (AA^\top)^{-1} \bar{y}_{t,k}] = 0.$$

Note that since  $A^\top$  is of dimension  $M$ -by- $N$ , this defines an under-determined system of equations. In other words, any  $\mu^*$  that satisfies

$$(AA^\top)^{-1} A\mu^* = (AA^\top)^{-1} \bar{y}_{t,k} + c,$$

for a vector  $c \in \mathbb{R}^N$  that lies in the null space of  $A$ :  $A^\top c = 0$ , will be a maximum likelihood estimator for the post-change mean. In particular, we may choose the zero vector  $c = 0$ , and use the estimator such that to form the GLR statistic.

$$(AA^\top)^{-1} A\mu^* = (AA^\top)^{-1} \bar{y}_{t,k}. \quad (8)$$

Substituting such a  $\mu^*$  into (6), we form the log-GLR. Using (8), the first and second terms in (6) become, respectively,

$$\begin{aligned} \bar{y}_{k,t}^\top (AA^\top)^{-1} A\mu^* &= \bar{y}_{k,t}^\top (AA^\top)^{-1} \bar{y}_{t,k}, \\ \frac{1}{2} \mu^{*\top} A^\top (AA^\top)^{-1} A\mu^* &= \frac{1}{2} \bar{y}_{k,t}^\top (AA^\top)^{-1} \bar{y}_{t,k}. \end{aligned}$$

By combining above, finally (6) becomes

$$\ell(t, k, \mu^*) = \frac{t-k}{2} \bar{y}_{k,t}^\top (AA^\top)^{-1} \bar{y}_{k,t}. \quad (9)$$

Finally, we define a sketching procedure that stops whenever the log-GLR statistic raises above a threshold  $b > 0$ :

$$T = \inf\{t : \max_{t-w \leq k < t} \frac{t-k}{2} \bar{y}_{k,t}^\top (AA^\top)^{-1} \bar{y}_{k,t} > b\}. \quad (10)$$

Here  $w > 0$  is a window-size, i.e., we only consider the past  $w$  samples from the current time  $t$ . The role of the window-size is two-fold. On the one hand, it reduces the memory requirements to implement the detection procedure, and on the other hand, it effectively establishes a minimum level of change that we want to detect.

2) *Equivalent formulation of fixed projection sketching procedure:* We can further simplify the log-GLR statistic in (9) by using the singular value decomposition (SVD) of  $A$ . This facilitates the performance analysis in Section IV and leads into some insights into the structure of the log-GLR statistic. Let the SVD of  $A$  be given by

$$A = U\Sigma V^\top, \quad (11)$$

where  $U \in \mathbb{R}^{M \times M}$ ,  $\Sigma \in \mathbb{R}^{M \times M}$  is a diagonal matrix containing all non-zero singular values, and  $V \in \mathbb{R}^{N \times M}$ . Then  $(AA^\top)^{-1} = U\Sigma^{-2}U^\top$ , and we can write the log-GLR statistic (9) as

$$\ell(t, k, \mu^*) = \frac{t-k}{2} \bar{y}_{k,t}^\top U \Sigma^{-2} U^\top \bar{y}_{k,t}. \quad (12)$$

Substitution of the average statistic (5) into (12) results in

$$\frac{\left\| \Sigma^{-1} U^\top \left( \sum_{i=k+1}^t y_i \right) \right\|^2}{2(t-k)}.$$

Now define  $z_i \triangleq \Sigma^{-1} U^\top y_i$ . Since under the null hypothesis  $y_i \sim \mathcal{N}(0, AA^\top)$ , so  $z_i \sim \mathcal{N}(0, I_M)$ . Similarly, under the alternative hypothesis  $y_i \sim \mathcal{N}(A\mu, AA^\top)$ , so  $z_i \sim \mathcal{N}(V^\top \mu, I_M)$ . Thus we have the following equivalent form for the sketching procedure in (10):

$$T' = \inf \{t : \max_{t-w \leq k < t} \frac{\left\| \sum_{i=k+1}^t z_i \right\|^2}{2(t-k)} > b\}. \quad (13)$$

This form of the sketching procedure has one intuitive explanation: it essentially projects the data into  $M$  (less than  $N$ ) independent data streams, and detects the change by forming a log-GLR statistic using these independent data streams.

## B. Time-varying projection

1) *Derivation of GLR statistic:* Similarly, we can derive the log-LR statistic for an assumed value of the change-point  $\kappa = k$  and observations accumulated up to time  $t$ :

$$\begin{aligned} \ell(t, k, \mu) &= \sum_{i=k+1}^t [y_i^\top (A_i A_i^\top)^{-1} A_i \mu - \frac{1}{2} \mu^\top A_i^\top (A_i A_i^\top)^{-1} A_i \mu]. \end{aligned} \quad (14)$$

Similarly, we may replace the unknown  $\mu$  with a maximum likelihood estimator using data in a time window  $[k+1, t]$ . Taking the derivative of  $\ell(t, k, \mu)$  in (14) with respect to  $\mu$  and setting it to zero, we obtain an equation for the maximum likelihood estimate  $\mu^*$

$$\left[ \sum_{i=k+1}^t A_i^\top (A_i A_i^\top)^{-1} A_i \right] \mu^* = \sum_{i=k+1}^t A_i^\top (A_i A_i^\top)^{-1} y_i. \quad (15)$$

To solve for  $\mu^*$  from the above, one needs to discuss the rank of the matrix  $\sum_{i=k+1}^t A_i^\top (A_i A_i^\top)^{-1} A_i$  in (15). Define the SVD of  $A_i = U_i D_i V_i^\top$  with  $U_i \in \mathbb{R}^{M_i \times M_i}$ ,  $D_i \in \mathbb{R}^{M_i \times M_i}$

and  $V_i \in \mathbb{R}^{N \times M_i}$ . We have that

$$\sum_{i=k+1}^t A_i^\top (A_i A_i^\top)^{-1} A_i = \sum_{i=k+1}^t V_i V_i^\top = Q Q^\top, \quad (16)$$

where  $Q = [V_{k+1}, \dots, V_t] \in \mathbb{R}^{N \times S}$  and  $S = \sum_{i=k+1}^t M_i$ . Consider two cases where

- (i)  $A_i$ 's are independent Gaussian random matrices. Note that in this case, the columns within each  $V_i$  in (16) are linearly independent with probability one. Moreover, the columns in different  $V_i$  blocks are independent since  $V_i$ 's are independent, and their entries are drawn as independent continuous random variables. Therefore, the columns of  $Q$  are linearly independent and  $\text{rank}(Q Q^\top) = \min(N, (t-k)M)$  with probability one. Hence, we can claim that if  $t-k < N/M$ ,  $Q Q^\top$  is rank deficient with probability 1; if  $t-k \geq N/M$ ,  $Q Q^\top$  is full rank with probability one;
- (ii)  $A_i$ 's are independent random matrices with entries drawn from a discrete distribution. In this case, we can also claim that if  $t-k < N/M$ ,  $Q Q^\top$  is not full rank and if  $t-k \geq N/M$ ,  $Q Q^\top$  is full rank with high probability, however, not with probability one.

Below, to avoid the issue of invertibility, we use the pseudo-inverse of the matrix in (16) and define

$$B_{k,t} \triangleq \left( \sum_{i=k+1}^t A_i^\top (A_i A_i^\top)^{-1} A_i \right)^\dagger \in \mathbb{R}^{N \times N},$$

then from (15),  $\mu^*$  is given by

$$\mu^* = B_{k,t} \sum_{i=k+1}^t A_i^\top (A_i A_i^\top)^{-1} y_i.$$

Substituting such a  $\mu^*$  into (14), we obtain the log-GLR statistic for time-varying projection:

$$\begin{aligned} \ell(t, k, \mu^*) &= \left( \sum_{i=k+1}^t A_i^\top (A_i A_i^\top)^{-1} y_i \right)^\top B_{k,t} \left( \sum_{i=k+1}^t A_i^\top (A_i A_i^\top)^{-1} y_i \right). \end{aligned} \quad (17)$$

One can detect a change, when the log-GLR statistic maximized over  $t-w < k < t$ , exceeds a threshold.

2) *Time-varying 0-1 project matrices:* We cannot further simplify the expression of GLR in (17) without specifying the form of  $A_t$ ,  $t = 1, 2, \dots$ . Below, we will focus on a special case when  $A_t$  has 0-1 entries only, which corresponds to the case that at each time we observe a subset of the entries or  $A_t$  corresponds to a sparse 0-1 matrix. With such 0-1 matrices, we can obtain a simpler expression for the statistic in (17).

In this case,  $A_t A_t^\top$  is an  $M_t$ -by- $M_t$  identity matrix, and  $A_t^\top A_t$  is a diagonal matrix. For a diagonal matrix  $D \in \mathbb{R}^{N \times N}$  with diagonal entries  $\lambda_1, \dots, \lambda_N$ , the pseudo-inverse of  $D$  is also a diagonal matrix with diagonal entries  $\lambda_i^{-1}$  if  $\lambda_i \neq 0$  and with diagonal entries 0 if  $\lambda_i = 0$ . Let the index set of the observed entries is  $\Omega_i$ . To simplify the form of the log-GLR,



we assume at each time  $i$ , we define indicator variables

$$\mathbb{I}_{in} = \begin{cases} 1, & \text{if } n \in \Omega_i; \\ 0, & \text{otherwise.} \end{cases} \quad (18)$$

Then the GLR statistic in (17) can be written as

$$\ell(t, k, \mu^*) = \sum_{n=1}^N \frac{\left( \sum_{i=k+1}^t [x_i]_n \mathbb{I}_{in} \right)^2}{\sum_{i=k+1}^t \mathbb{I}_{in}}, \quad (19)$$

Hence, for 0-1 sketching matrices, the sketching procedure becomes

$$T_{\{0,1\}} = \inf \left\{ t : \max_{t-w \leq k < t} \frac{1}{2} \sum_{n=1}^N \frac{\left( \sum_{i=k+1}^t [x_i]_n \mathbb{I}_{in} \right)^2}{\sum_{i=k+1}^t \mathbb{I}_{in}} > b \right\}, \quad (20)$$

where  $b > 0$  is the prescribed threshold. Note that the GLR statistic essentially computes the sum of each entries within the time window  $[t-w, t)$ , and then average the squared-sum over  $N$  dimensions.

#### IV. PERFORMANCE ANALYSIS

In this section, we present theoretical approximations two performance matrices, the average-run-length (ARL), which captures the false-alarm-rate, and the expected detection delay (EDD), which captures the power of the detection statistic, for the proposed procedures  $T$  and  $T_{\{0,1\}}$ .

##### A. Performance metrics

First, we introduce some notations. Under the null hypothesis  $H_0$  (1), the observations have zero mean. Probability and expectation in this case are denoted by  $\mathbb{P}^\infty$  and  $\mathbb{E}^\infty$ , respectively. Under the hypothesis  $H_1$ , alternatively, there exists a change-point  $\kappa$ ,  $0 \leq \kappa < \infty$  such that the observations have mean  $\mu$  for all  $t > \kappa$ . Probability and expectation in this case are denoted by  $\mathbb{P}^\kappa$  and  $\mathbb{E}^\kappa$ , respectively.

The choice of the threshold  $b$  involves a trade-off between two standard performance metrics that are commonly used for analyzing change-point detection procedures [25]: (i) the expected value of the stopping time when there is no change, the average run length (ARL); (ii) the expected detection delay (EDD), defined to be the expected stopping time in the extreme case where a change occurs immediately at  $\kappa = 0$ , which is denoted as  $\mathbb{E}^0\{T\}$ . The following argument from [26] explains why we consider  $\mathbb{E}^0\{T\}$ . When there is a change at  $\kappa$ , we are interested in the expected delay until its detection, i.e., the conditional expectation  $\mathbb{E}^\kappa\{T - \kappa | T > \kappa\}$ , which is a function of  $\kappa$ . When the shift in the mean only occurs in the positive direction  $[\mu]_i \geq 0$ , it can be shown that  $\sup_\kappa \mathbb{E}^\kappa\{T - \kappa | T > \kappa\} = \mathbb{E}^0\{T\}$ . It is not obvious that this remains true when  $[\mu]_i$  can be either positive or negative. However, since  $\mathbb{E}^0\{T\}$  is certainly of interest and reasonably easy to analyze, it is common to consider  $\mathbb{E}^0\{T\}$ .

##### B. Fixed projection

We can obtain approximations to the ARL and the EDD for the sketching procedure with a fixed projection as follows:

**Theorem 1** (ARL, fixed projection). Assume that  $1 \leq M \leq N$ ,  $b \rightarrow \infty$  with  $M \rightarrow \infty$  and  $b/M$  fixed. Then for  $w = o(b^r)$  for some positive integer  $r$ , we have that the ARL of the sketching procedure defined in (10) is given by

$$\mathbb{E}^\infty\{T\} = \frac{2\sqrt{\pi}}{c(M, b, w)} \frac{1}{1 - \frac{M}{2b}} \frac{1}{\sqrt{M}} \left( \frac{M}{2b} \right)^{\frac{M}{2}} e^{b - \frac{M}{2}} (1 + o(1)), \quad (21)$$

where

$$c(M, b, w) = \int_{\sqrt{\frac{2b}{w}(1 - \frac{M}{2b})}}^{\sqrt{2b}(1 - \frac{M}{2b})} u \nu^2(u) du, \quad (22)$$

and the special function

$$\nu(u) = 2u^{-2} \exp[-2 \sum_{i=1}^{\infty} i^{-1} \Phi(-|u| i^{1/2}/2)],$$

(cf. [27], page 82). For numerical purposes, a simple and accurate approximation is given by (cf. [28])

$$\nu(u) \approx \frac{2/u[\Phi(u/2) - 0.5]}{(u/2)\Phi(u/2) + \phi(u/2)}.$$

**Theorem 2** (EDD, fixed projection). Suppose  $b \rightarrow \infty$  with other parameters held fixed. Then for a given matrix  $A$  with right singular vectors  $V$ , the EDD of the sketching procedure (10) when  $\kappa = 0$  is given by

$$\mathbb{E}^0\{T\} = \frac{b + \rho(\Delta) - M/2 - \mathbb{E}\{\min_{t \geq 0} \tilde{S}_t\} + o(1)}{\Delta^2/2}. \quad (23)$$

where

$$\Delta = \|V^\top \mu\|. \quad (24)$$

Here  $\tilde{S}_t \triangleq \sum_{i=1}^t \delta_i$  is a random walk where the increments  $\delta_i$  are independent and identically distributed with mean  $\Delta^2/2$  and variance  $\Delta^2$ ,  $\mathbb{E}\{\min_{t \geq 0} \tilde{S}_t\} = -\sum_{i=1}^{\infty} \mathbb{E}\{\tilde{S}_i^-\}$  and  $(x)^- = -\min\{x, 0\}$ .

The proofs for the above two theorems utilize the equivalent form of  $T$  in (13), and draw a connection to the ‘‘mixture procedure’’ (cf.  $T_2$  in [25]) with parameter  $p_0 = 1$ ,  $M$  sensors, and the post-change mean vector is given by  $V^\top \mu$ . This means that under the null hypothesis that there is no change, the sketching procedure is equivalent to monitoring  $M$  independent zero-mean noise sources with unit variance; under the alternative hypothesis that there is a change, the post-change distribution is Gaussian with mean shifted to  $V^\top \mu$  and variance remains the same.

**Remark 1.** The first order approximation to the EDD in Theorem 2 is  $b/(\Delta^2/2)$ : the threshold  $b$  divided by the Kullback-Leibler (K-L) divergence (see, e.g., [25] for the fact that  $\Delta^2/2$  is the K-L divergence between  $\mathcal{N}(0, I_M)$  and  $\mathcal{N}(V^\top \mu, I_M)$ ). This is consistent with intuition since the expected increment of the detection statistics is roughly the K-L divergence of the test.

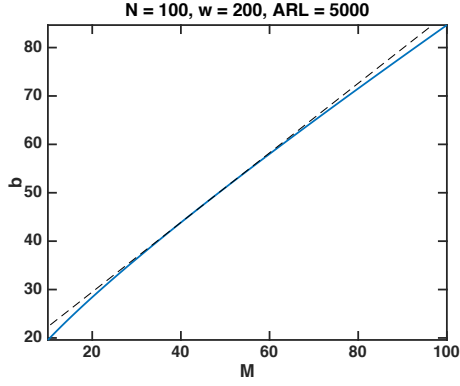


Fig. 1. For a fixed ARL being 5000, the curve for threshold  $b$  versus  $M$  (obtained using approximation in Theorem 1), when  $N = 100$  and  $w = 200$ . Dashed is a tangent line of the curve.

*Remark 2.* For a fixed large ARL, when  $M$  increases, the corresponding threshold  $b$  grows approximately linearly with  $M$ . This is a useful fact for establishing our subsequent result in Section V. It is verified numerically in Fig. 1 when  $N = 100$ ,  $w = 200$ , for a fixed ARL to be 5000, and the corresponding threshold  $b$  is found using Theorem 1, when  $M$  increases from 10 to 100. (In Section VI, we verify that Theorem 1 is an accurate approximation.)

More precisely, this fact can be derive from Theorem 1, as following corollary

*Corollary 1.* Assume a large constant  $\gamma \in (e^5, e^{20})$ . Let  $w \geq 100$ . For any large enough  $M > 24.85$ , the threshold  $b$  such that the corresponding  $\text{ARL } \mathbb{E}^\infty\{T\}$  is equal to  $\gamma$  satisfies  $M/b \in (0.5, 2)$ . In other words,  $\max\{M/b, b/M\} \leq 2$ .

1) *Accuracy of theoretical approximations:* Consider  $A$  generated as a Gaussian random matrix, with entries i.i.d.  $\mathcal{N}(0, 1/N)$ . We use Theorem 1 to find the threshold  $b$  corresponding to an ARL equal to 5000. Since the ARL is an increasing function of the threshold  $b$ , we use bisection to find the threshold  $b$  that corresponds to a targeted ARL 5000. Then we compare it with a threshold  $b$  that is found from simulation. As shown in Table I, the threshold find using Theorem 1 is very close to that obtained from simulation. Therefore, even if these theoretical ARL approximation is derived in an asymptotic regime when  $N$  tends to infinity, it is applicable when  $N$  is large but finite. This is quite useful in determining a threshold for a targeted ARL, as simulations for large  $N$  and  $M$  can be quite time-consuming, for a large ARL (e.g., 5000 or 10,000).

Moreover, we also simulate the EDD detecting a signal with a post-change mean vector  $\mu$  with entries all equal to  $[\mu]_i = 0.5$ . As also shown in Table I, the approximations for EDD using Theorem 2 are also accurate.

We have also verified the theoretical approximations are accurate for the expander graphs (details omitted).

### C. Time-varying 0-1 random projection matrices

Below, we obtain approximations to ARL and EDD with time-varying projections with 0-1 entries and fixed dimensions  $M_t = M$ . Assume at each time  $t$ , we randomly sample

TABLE I

$A$  BEING A FIXED GAUSSIAN RANDOM MATRIX.  $N = 100$ ,  $w = 200$ ,  $\text{ARL} = 5000$ , FOR SIMULATED EDD  $[\mu]_i = 0.5$ . NUMBERS IN THE PARENTHESES ARE THE STANDARD DEVIATION OF THE SIMULATED EDD.

$M$	$b$ (theo)	$b$ (simu)	EDD (theo)	EDD (simu)
100	84.65	84.44	3.4	4.3 (0.9)
70	64.85	64.52	4.0	5.1 (1.2)
50	51.04	50.75	4.8	5.9 (1.6)
30	36.36	36.43	7.7	7.6 (2.5)
10	19.59	19.63	19.8	17.4 (9.8)

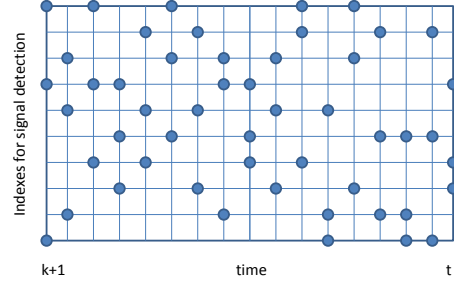


Fig. 2. A sampling scheme realization when  $A_t$  is a 0-1 matrix. Each dot denotes a sampled observation.

$M$  out of  $N$  dimensions of the signal to observe. Hence, at each time, each signal dimension has a probability

$$r = M/N \in (0, 1)$$

of being sampled. The sampling scheme is illustrated in Fig. 2, when there are  $N = 10$  dimensions,  $M = 3$  entries are sampled at each time (the number of the dots in each column is 3) over 17 consecutive time period from time  $k = t - 17$  to time  $t$ . For such a sampling scheme, we have the following result

*Theorem 3* (ARL, time-varying 0-1 random projection). Let  $r = M/N$ . When  $b \rightarrow \infty$ , for  $b' = b/r$ , for the procedure defined in (20) we have that

$$\begin{aligned} & \mathbb{E}^\infty\{T_{\{0,1\}}\} \\ & \approx \frac{2\sqrt{\pi}}{c(N, b', w)} \frac{1}{\sqrt{N}} \frac{1}{1 - \frac{N}{2b'}} \left(\frac{N}{2}\right)^{\frac{N}{2}} b'^{-\frac{N}{2}} e^{b' - \frac{N}{2}}, \end{aligned} \quad (25)$$

where  $c(N, b', w)$  is defined by replacing  $b$  with  $b'$  in (22).

The approximation is obtained by asymptotic analysis and replacing the detection statistic by its mean over random sampling conditioning on the data.

We can also obtain the first order approximation of EDD for  $T_{\{0,1\}}$ . The idea is to relax the constraint that each time we observe exactly  $M$  out of  $N$  entries, by assuming a random sampling scheme that independently sample each entry of  $x_i$  with probability  $r$ , for  $1 \leq n \leq N$ . Define i.i.d. Bernoulli random variables  $\xi_{ni}$  with parameter  $r$  for  $1 \leq n \leq N$  and

$i \geq 1$  and let

$$Z_{n,k,t} \triangleq \frac{\sum_{i=k+1}^t [x_i]_n \xi_{ni}}{\sqrt{(t-k)r}}.$$

Based on this, introduce a procedure whose behavior is arguably similar to  $T_{\{0,1\}}$

$$T'_{\{0,1\}} = \inf\{t \geq 1 : \max_{t-w \leq k < t} \frac{1}{2} \sum_{n=1}^N Z_{n,k,t}^2 > b\},$$

where  $b > 0$  is the prescribed threshold. To obtain EDD approximation to  $T'_{\{0,1\}}$ , first note that

$$\mathbb{E}^0\{Z_{n,0,t}^2\} = \frac{(rt\mu_n)^2 + rt + rt\mu_n^2}{rt} = 1 + (rt+1)\mu_n^2. \quad (26)$$

For a sufficiently large window size  $w$ , we have that

$$\mathbb{E}^0\left\{\max_{k < t} \frac{1}{2} \sum_{n=1}^N Z_{n,k,t}^2\right\} \approx N/2 + (rt+1) \sum_{n=1}^N \mu_n^2/2. \quad (27)$$

Using Wald's identity [27] and ignoring the overshoot of the statistic over the threshold  $b$ , we obtain a first order approximation by equating the right-hand side of (27) to  $b$ , taking expectations on both sides:

$$N/2 + \mathbb{E}^0\{T'_{\{0,1\}}\} \left(r \sum_{n=1}^N \mu_n^2/2\right) + \sum_{n=1}^N \mu_n^2/2 = b,$$

from which we can solve for

$$\mathbb{E}^0\{T'_{\{0,1\}}\} \approx \left(\frac{2b-N}{\sum_{n=1}^N \mu_n^2} - 1\right) \cdot \frac{N}{M}. \quad (28)$$

1) *Accuracy of theoretical approximations:* Table II shows the accuracy of the approximation of  $b$ 's using the ARL in (25) and the accuracy of the approximation of EDD in (28) with various  $M$ 's if  $N = 100$ ,  $w = 200$ , when all  $[\mu]_i = 0.5$ .

TABLE II  
A<sub>i</sub>'S BEING TIME-VARYING.  $N = 100$ ,  $w = 200$ , ARL = 5000, FOR SIMULATED EDDs ALL  $[\mu]_i = 0.5$ . NUMBERS IN THE PARENTHESES ARE STANDARD DEVIATION OF THE SIMULATED RESULTS.

$M$	$b$ (theo)	$b$ (simu)	EDD (theo)	EDD (simu)
100	84.65	84.44	2.8	3.3 (0.8)
70	83.72	83.41	3.8	4.5 (1.2)
50	82.84	83.02	5.3	6.1 (1.5)
30	81.46	82.48	8.7	9.8 (2.4)
10	78.32	79.27	23.4	26.6 (6.4)

## V. PERFORMANCE-COMPLEXITY TRADE-OFF

There is a trade-off in performance and complexity for sketching procedure. The trade-off is in the sense that when more sketches are used (in the extreme case,  $M = N$ ), performance will be better, however, at the cost of higher complexity (less dimensionality reduction, more entries need to be observed, etc.). In this section, we characterize such trade-off and show that the performance loss of using sketching can

be bounded. To facilitate presentation, in the following, we focus on fixed projection.

### A. Relative performance metric

We consider a relative performance metric, which is the ratio of EDD using the original data (denoted as  $\text{EDD}(N)$ , which corresponds to letting  $A = I$ ) and EDD using the sketches (denoted as  $\text{EDD}(M)$ ). We will show that this ratio depends critically on the following quantity

$$\Gamma \triangleq \frac{\|V^\top \mu\|^2}{\|\mu\|^2}. \quad (29)$$

From Theorem 2, we have that the EDD of the sketching procedure  $\mathbb{E}^0\{T\}$  is  $2b/\|V^\top \mu\|^2(1 + o(1))$ . Define  $Q_M = M/b_M$ ,  $Q_N = N/b_N$  and  $b_M$  and  $b_N$  are the thresholds such that  $\mathbb{E}^\infty\{T\} = 5000$ , respectively. Then, the ratio is approximately

$$\frac{\text{EDD}(N)}{\text{EDD}(M)} \approx \frac{N}{M} \cdot \frac{\|V^\top \mu\|^2}{\|\mu\|^2} = \frac{N}{M} \cdot \frac{Q_M}{Q_N} \cdot \Gamma. \quad (30)$$

Using Corollary 1, we have  $Q_M \in (0.5, 2)$  and  $Q_N \in (0.5, 2)$ , then the ratio is between  $(1/4) \cdot (N/M) \cdot \Gamma$  and  $4 \cdot (N/M) \cdot \Gamma$ . Next, we bound  $\Gamma$  when  $A$  is a Gaussian matrix and an expander graph, respectively.

### B. Bounding $\Gamma$

1) *Gaussian matrix:* Consider  $A \in \mathbb{R}^{M \times N}$  whose entries are i.i.d. Gaussian with mean zero and variance  $1/M$ .

*Lemma 1 ([29]).* Let  $A \in \mathbb{R}^{M \times N}$  have i.i.d.  $\mathcal{N}(0, 1)$  entries, and its SVD be given by  $A = U\Sigma V^\top$ . Then for any fixed vector  $\mu$ ,

$$\Gamma \sim \text{Beta}\left(\frac{M}{2}, \frac{N-M}{2}\right). \quad (31)$$

More related results can be found in [30]. Since the  $\text{Beta}(\alpha, \beta)$  distribution has mean  $\alpha/(\alpha + \beta)$ , we have

$$\mathbb{E}\{\Gamma\} = \frac{M/2}{M/2 + (N-M)/2} = \frac{M}{N}.$$

We may also show that, provided  $M$  and  $N$  grow proportionally,  $\Gamma$  converges to its mean value at a rate exponential in  $N$ . Define  $\delta \in (0, 1)$  to be

$$\delta \triangleq \lim_{N \rightarrow \infty} \frac{M}{N}. \quad (32)$$

*Theorem 4 (Gaussian  $A$ ).* Let  $A \in \mathbb{R}^{M \times N}$  have entries i.i.d.  $\mathcal{N}(0, 1)$ . Let  $N \rightarrow \infty$  such that (32) holds. Then for  $0 < \epsilon < \min(\delta, 1 - \delta)$ ,

$$\mathbb{P}\{\delta - \epsilon < \Gamma < \delta + \epsilon\} \rightarrow 1, \quad (33)$$

at a rate exponential in  $N$ .

2) *Sparse sketching matrix  $A$ :* Interestingly, we can be shown that for certain sparse 0-1 matrices  $A$  (in particular, the expander graphs),  $\Gamma$  is also bounded. This holds for the "one-sided" signals, i.e., the post-change mean vector is element-wise positive. This scenario is typically considered

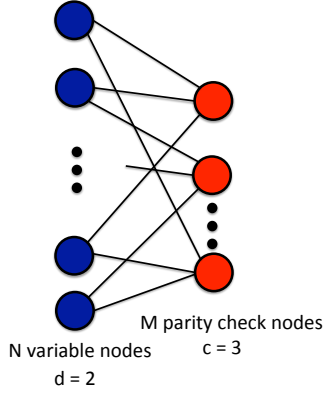


Fig. 3. Illustration of a bipartite graph with  $d = 2$  and  $c = 3$ . Following coding theory terminology, we call the left variables nodes (there are  $N$  such variables), which correspond to the entries of  $x_t$ , and we call the right variables parity check nodes (there are  $M$  such nodes), which correspond to entries of  $y_t$ . In a bipartite graph, connections between the variable nodes are not allowed. The adjacency matrix of the bipartite graph corresponds to our  $A$  here.

in environmental monitoring [25]. These sparse sketching matrices  $A$  enable efficient sketching schemes, as each entry in the sketching vector only requires collecting information from few dimensions of the original data vector.

Assume  $[\mu]_i \geq 0$  for all  $i$ . Let  $A \in \mathbb{R}^{M \times N}$  consisting of binary entries, which corresponds to a bipartite graph, illustrated in Fig. 3. We further consider a bipartite graph with regular left degree  $c$  (i.e., the number of edges from each variable node is  $c$ ), and regular right degree  $d$  (i.e., the number of edges from each parity check node is  $d$ ), as illustrated in Fig. 3. Hence, this requires  $Nc = Md$ .

Expander graphs satisfy the above requirements, and they have been used in compressed sensing to sense a sparse vector (e.g. [31]). In particular, a matrix  $A$  corresponds to a  $(s, \epsilon)$ -expander graph with regular right degree  $d$  if and only if each column of  $A$  has exactly  $d$  “1”s, and for any set  $S$  of right nodes with  $|S| \leq s$ , the set of neighbors  $\mathcal{N}(S)$  of the left nodes has size  $|\mathcal{N}(S)| \geq (1 - \epsilon)d|S|$ . If it further holds that each row of  $A$  has  $c$  “1”s, we say  $A$  corresponds to a  $(s, \epsilon)$ -expander with regular right degree  $d$  and regular left degree  $c$ . The existence of such expander graphs is established in [32]:

**Lemma 2** ([32]). For any fixed  $\epsilon > 0$  and  $\rho \triangleq M/N < 1$ , when  $N$  is sufficiently large, there always exists an  $(\alpha N, \epsilon)$  expander with a regular right degree  $d$  and a regular left degree  $c$  for some constants  $\alpha \in (0, 1)$ ,  $d$  and  $c$ .

**Theorem 5** (Expander  $A$ ). If  $A$  corresponds to a  $(s, \epsilon)$ -expander with regular degree  $d$  and regular left degree  $c$ , for any nonnegative vector  $[\mu]_i \geq 0$ , we have

$$\Gamma \geq \frac{M(1 - \epsilon)}{dN}.$$

### C. Consequence

Above, we have shown that when  $A$  is a Gaussian random matrix,  $\Gamma$  is on the order of  $M/N$ . Hence, for Gaussian

random matrix, the ratio (30) is between  $1/4$  and  $4$  if the conditions in Corollary 1 are satisfied. This result is intriguing since it implies that the performance loss is bounded by a small constant, which is also observed from our numerical examples.

Moreover, when  $A$  is a sparse 0-1 matrix with  $d$  non-zero entries on each row (in particular, an expander graph),  $\Gamma$  is greater than  $M(1 - \epsilon)/(dN)$ . Hence, from the ratio (30), this mean that when Corollary 1 holds,  $\text{EDD}(M)$  is approximately at most a factor times  $\text{EDD}(N)$ , where the factor is between  $(1/4) \cdot d/(1 - \epsilon)$  and  $4d/(1 - \epsilon)$  for some small number  $\epsilon > 0$ .

There is one possible intuitive explanation. Unlike in compressed sensing, where our goal is to recover a sparse signal, and hence one needs the projection to preserve norm up to a factor through the restricted isometry property (RIP) [33], here our goal is to detect a non-zero vector in Gaussian noise. Hence, even though the projection reduces the norm of the vector, as long as the projection does not diminish the signal normal to be below the noise floor, we are still able to detect it.

## VI. NUMERICAL EXAMPLES

We compare our sketching procedure with a GLR procedure using the original data (by letting  $A = I$  in the sketching procedure) similar to what we did earlier in Section V-A, and then compare it with a standard multivariate CUSUM for sketches.

In the subsequent examples, we select ARL to be 5000 to represent a low rate of false detection (similar choice has been made in other sequential change-point detection work such as [25]). In practice, however, the target ARL value depends on the sampling frequency and how frequent we can tolerate false detection (once a month or once a year). Below,  $\text{EDD}_0$  denotes the EDD when  $A = I$  (i.e., no sketching is used). All simulated results are obtained from  $10^4$  repetitions.

### A. Fixed projection, Gaussian random matrix

First consider Gaussian  $A$  with  $N = 500$  and different number of sketches  $M < N$ .

1) *EDD versus signal magnitude*: Assume the post-change mean vector has entries with equal magnitude:  $[\mu]_i = \mu_0$ . Fig. 4(a) shows EDD versus an increasing signal magnitude  $\mu_0$ . We find that when  $\mu_0$  is sufficiently large, the sketching procedure can approach the performance of the procedure using the full data. Table III shows the minimum  $M$  required so that the  $\text{EDD}(M)$  of the sketching procedure is less than  $1 + \text{EDD}(N)$ , where  $\text{EDD}(N)$  is when full data is used, in Fig. 4(a). We find that when  $\mu_0$  is sufficiently large, we may even use  $M$  less than 30 for a  $N = 500$  to have little performance loss. Note that here we do not require signals to be sparse.

2) *EDD versus signal sparsity*: Then we assume that the post-change mean vector is sparse: only  $100p\%$  entries  $\mu_i$  being one and the other entries being zero. Fig. 4(b) shows EDD versus an increasing  $p$ . As  $p$  increases, the signal strength also increases, and the sketching procedure approaches the performance using the full data. Similarly, we



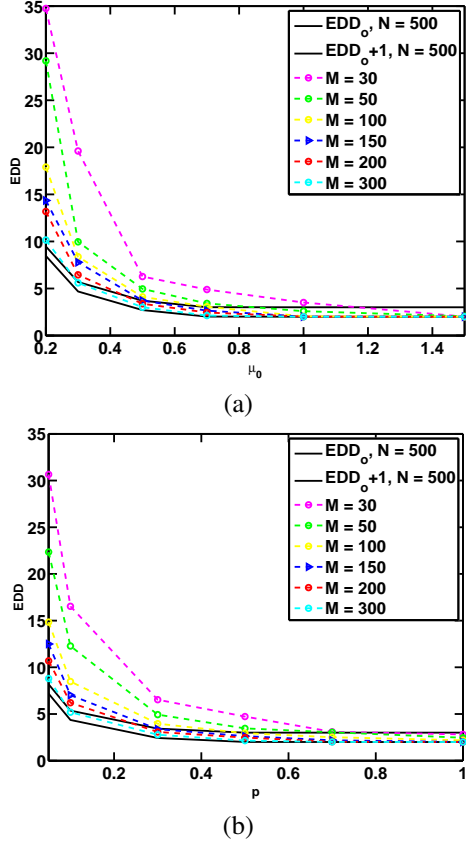


Fig. 4.  $A$  being a fixed Gaussian random matrix. The standard deviation of each point is less than half of its value. (a) EDD versus  $\mu_0$ , when all  $[\mu]_i = \mu_0$ ; (b) EDD versus  $p$  when we randomly select 100% entries  $[\mu]_i$  to be one and set the other entries to be zero; the smallest value of  $p$  is 0.05.

TABLE III

$A$  BEING A FIXED GAUSSIAN RANDOM MATRIX. MINIMUM  $M_*$  REQUIRED FOR VARIOUS MEAN SHIFTS  $\mu_0$ .  $N = 500$ ,  $w = 200$  AND ALL  $[\mu]_i = \mu_0$ . NUMBERS IN THE PARENTHESES ARE STANDARD DEVIATION OF THE SIMULATED RESULTS.

$\mu_0$	0.3	0.5	0.7	1	1.2
$M_*$	300	150	100	50	30
EDD <sub>0</sub>	8.5 (2.0)	4.7 (0.9)	2.7 (0.5)	2.0 (1.1)	2 (0.01)

obtain the minimum  $M$  required so that the  $\text{EDD}(M)$  of the sketching procedure is less than  $1 + \text{EDD}(N)$ . For example, when  $p = 0.5$ , one can use  $M = 100$  for a  $N = 500$  without much performance loss.

### B. Fixed projection, expander graph

Now assume  $A$  being an expander graph with  $N = 500$  and different number of sketches  $M < N$ . We run the simulations with the same settings as those in Section VI-A.

1) *EDD versus signal magnitude*: Assume the post-change mean vector  $[\mu]_i = \mu_0$ . Fig. 5(a) shows EDD with an increasing  $\mu_0$ . Note that the simulated EDDs are smaller than those for the Gaussian random projections in Fig. 4. A possible reason is that the expander graph is better at aggregating the signals when  $[\mu]_i$  are all positive. However,

when  $[\mu]_i$  are can be either positive or negative, the two choices of  $A$  have similar performance, as shown in Fig. 6, where  $[\mu]_i$  are drawn i.i.d. uniformly from  $[-3, 3]$ .

2) *EDD versus signal sparsity*: Then, assume that the post-change mean vector has only 100% entries  $\mu_i$  being one and the other entries being zero. Fig. 5(b) shows the simulated EDD versus an increasing  $p$ . As  $p$  tends to 1, the sketching procedure approaches the performance using the full data. From Fig. 5(b) we can obtain the minimum  $M$  required so that the  $\text{EDD}(M)$  of the sketching procedure is less than  $1 + \text{EDD}(N)$ , as shown in Table IV. For example, when  $p$  is around 0.5, we may use  $M = 50$  for a  $N = 500$  without much performance loss. When  $p$  is larger than 0.7, one may use  $M$  less than 30 for a  $N = 500$ .

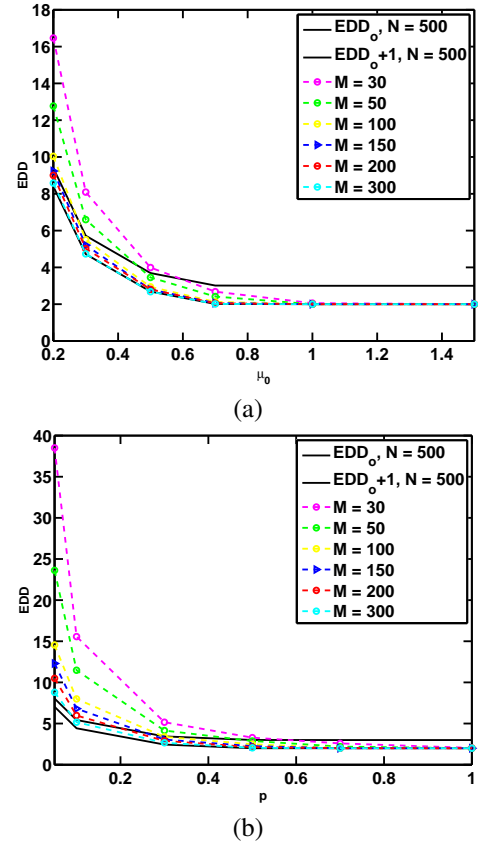


Fig. 5.  $A$  being a fixed expander graph. The standard deviation of each point is less than half of its value. (a) EDD versus  $\mu_0$ , when all  $[\mu]_i = \mu_0$ ; (b) EDD versus  $p$  when we randomly select 100% entries  $[\mu]_i$  to be one and set the other entries to be zero; the smallest value of  $p$  is 0.05.

TABLE IV

$A$  BEING A FIXED EXPANDER GRAPH. MINIMUM  $M_*$  REQUIRED FOR VARIOUS  $p$ .  $N = 500$ ,  $w = 200$  AND 100% OF ENTRIES  $[\mu]_i = 1$ . NUMBER IN PARENTHESES ARE STANDARD DEVIATION OF THE SIMULATED RESULTS.

$p$	0.1	0.2	0.3	0.5	0.7
$M_*$	300	200	100	50	30
EDD <sub>0</sub>	4.4 (0.8)	2.4 (0.5)	2.0 (0.1)	2.0 (0.02)	2.0 (0.01)

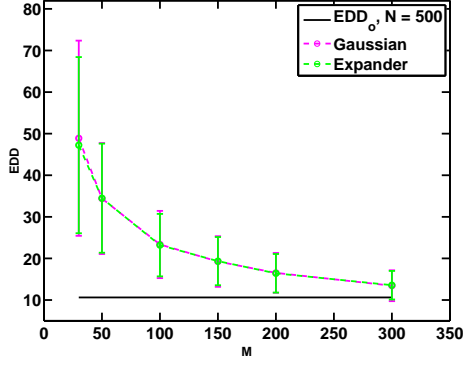


Fig. 6. Comparison of EDDs for  $A$  being a Gaussian random matrix versus an expander graph, when  $[\mu]_i$ 's are i.i.d. generated from  $[-3, 3]$ .

### C. Time-varying projections with 0-1 matrices

To demonstrate the performance of the procedure (20) using time-varying projection with 0-1 entries, we again consider two cases: the post-change mean vector  $[\mu]_i = \mu_0$  and the post-change mean vector has 100% entries  $[\mu]_i$  being one and the other entries being zero.

The simulated EDDs are shown in Fig. 7. Note that (20) can detect change quickly with a small subset of observations. Although EDDs of (20) are larger than those for the fixed projections in Fig. 4 and Fig. 5, this example shows that projection with 0-1 entries can have little performance loss in some cases, and it is still a viable candidate since such projection means simpler measurement scheme.

### D. Comparison with multivariate CUSUM

We compare our sketching method with a benchmark approach adapted from the classic multivariate CUSUM procedure [34] that applies directly to sketches. Hence, this does not incorporate the covariance structure of the sketches. Moreover, in multivariate CUSUM, one needs a prescribed post-change mean vector (which is set to be an all-one vector in our example). Hence, its performance may be affected by parameter misspecification. We compare the performance again in two settings, when all  $[\mu]_i$  are equal to a constant, and when 100% entries of the post-change mean vector are positive valued. In Fig. 8, the sketching procedure has a significant performance gain relative to standard multivariate CUSUM.

## VII. REAL-WORLD EXAMPLES

### A. Solar flare detection

We use our method to detect a solar flare in a video sequence from the Solar Data Observatory (SDO)<sup>1</sup>. Each frame is of size  $232 \times 292$  pixels, which results in an ambient dimension  $N = 67744$ . In this example, the normal frames are slowly drifting background sun surfaces, and the anomaly is a much brighter transient solar flare emerges at  $t = 223$ .

<sup>1</sup>The video can be found at <http://nislabs.ee.duke.edu/MOUSSE/>. The Solar Object Locator for the original data is SOL2011-04-30T21-45-49L061C108.

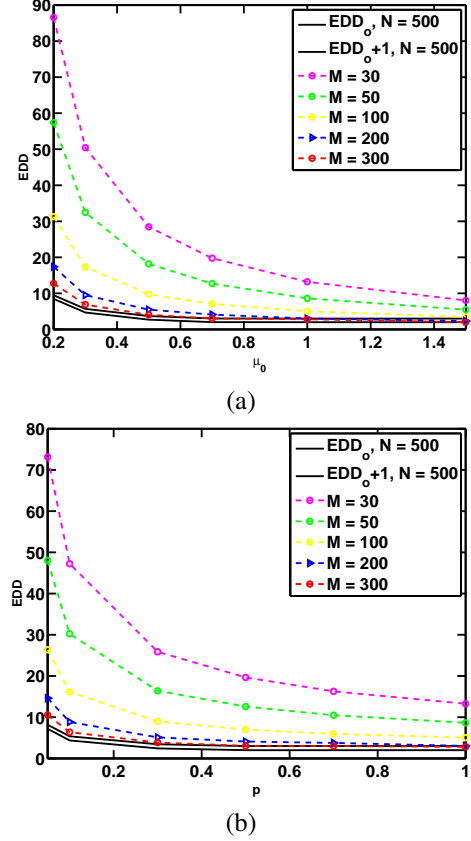


Fig. 7.  $A_t$ 's are time-varying projection. The standard deviation of each point is less than half of its value. (a) EDD versus  $\mu_0$ , when all  $[\mu]_i = \mu_0$ ; (b) EDD versus  $p$  when we randomly select 100% entries  $[\mu]_i$  to be one and set the other entries to be zero; the smallest value of  $p$  is 0.05.

Fig. 9(a) is a snapshot of the original SDO data at  $t = 150$  before the solar flare emerges, and Fig. 9(b) is a snapshot at  $t = 223$  when the solar flare emerges as a brighter curve in the middle of the image. We first preprocess the data by tracking and removing the slowly changing background with the MOUSSE algorithm [35] to obtain tracking residuals. The Gaussianity for the residuals, which corresponds to our  $x_t$ , is verified by the one-sample Kolmogorov-Smirnov test. For instance, the p-value is 0.47 for the signal at  $t = 150$ , which indicates that the Gaussianity is a reasonable assumption.

We apply the sketching procedure with fixed projection to the MOUSSE residuals for dimensionality reduction. Choosing the sketching matrix  $A$  to be an  $M$ -by- $N$  Gaussian random matrix with entries i.i.d.  $\mathcal{N}(0, 1/N)$ . Note that the signal is deterministic in this case. To evaluate our method, we run the procedure 500 times, each time using a different random Gaussian matrix as the fixed projection  $A$ . Fig. 10 shows the error-bars of the EDDs from 500 runs. As  $M$  increases, both the means and standard deviations of the EDDs decrease. When  $M$  is larger than 750, the EDD is less than 3 with a very high chance, which means that our sketching detection procedure can reliably detect the solar flare with only 750 sketches. This is a significant reduction compared with using the original data with a dimensionality

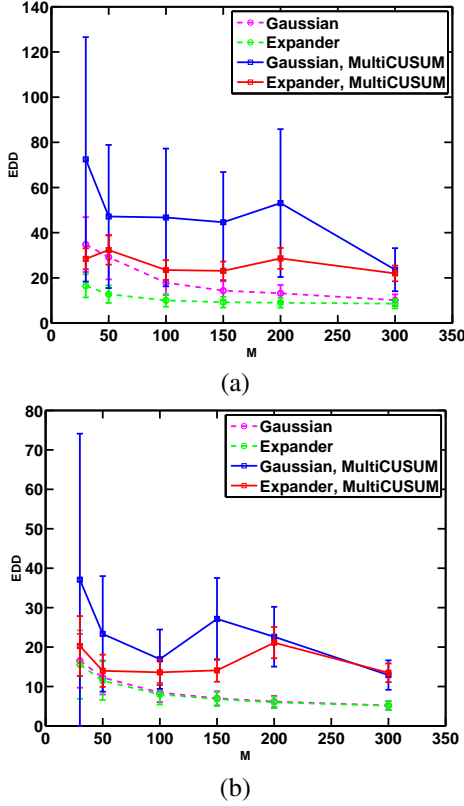


Fig. 8. Comparison of the sketching procedure with a method adapted from multivariate CUSUM. (a) EDDs versus various  $M$ s, when all  $[\mu]_i = 0.2$ ; (b) EDDs versus various  $M$ s, when we randomly select 10% entries  $[\mu]_i$  to be one and set the other entries to be zero.

reduction ratio of  $750/67744 \approx 0.01$ .

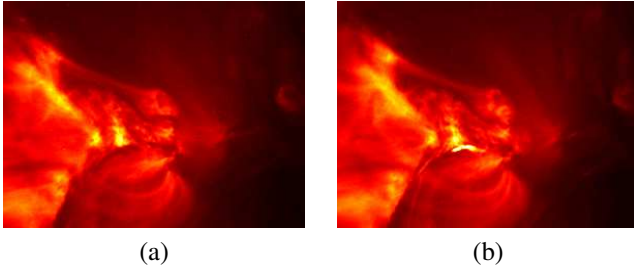


Fig. 9. Snapshot of the original solar flare data. (a) at  $t = 150$ ; (b) at  $t = 223$ . The true change-point location is  $t = 223$ .

### B. Power system

Finally, we present a synthetic example based on the real power network topology of the Western States Power Grid of the United States, which consists of 4941 nodes and 6594 edges and the minimum degree of a node in the network is 1, as shown in Fig. 11<sup>2</sup>. The nodes represent generators, transformers, and substations, and edges represent high-voltage transmission lines between them [36]. Note that

<sup>2</sup>The topology of the power network can be downloaded at <http://networkdata.ics.uci.edu/data/power/> [36].

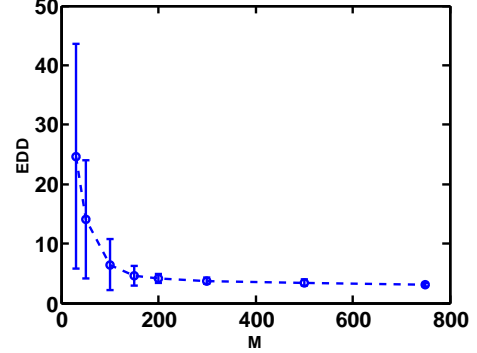


Fig. 10. Solar flare detection: EDD versus various  $M$  when  $A$  is an  $M$ -by- $N$  Gaussian random matrix. The error-bars are obtained from  $10^4$  repetitions with runs with different Gaussian random matrix  $A$ .

the graph is sparse and that there are many “communities” which correspond to densely connected subnetworks.

In this example, we simulate a situation for power failure over this large network. Assume at each time we may observe the real power injection at an edge. When the power system is in steady state, the observation is the true state plus Gaussian observation noise [37]. We may estimate the true state (e.g., using techniques in [37]), subtract it from the observation vector, and treat the residual vector as our signal  $x_i$ , which can be assumed to be i.i.d. standard Gaussian distribution. When failures happen in a power system, there will be a shift in the mean for a small number of affected edges, since in practice, when there is a power failure, usually only a small part of the network is affected simultaneously.

To perform sketching, each time, we randomly choose  $M$  nodes in the network and measure the sum of the quantities over all attached edges as shown in Fig. 12. This corresponds to  $A'_t$ s with  $N = 6594$  and various  $M < N$ . Note that in this case, our projection matrix is a 0-1 matrix whose structure is constrained by the network topology. Although our example is a highly simplified model for power networks, it sheds some light on the potential of our method applied to monitoring real power networks.

In the following experiment, we assume that the means of 5% of the edges in the network increase by  $\mu_0$ . Set the threshold  $b$  such that the ARL is 5000. Fig. 13 shows the simulated EDD versus an increasing signal strength  $\mu_0$ . Note that the EDD using a small number of sketches is quite small if  $\mu_0$  is sufficiently large. For example, when  $\mu_0 = 4$ , one may detect the change by observing from only  $M = 100$  sketches, which is a significant reduction compared with using the original data with a ratio of  $100/4941 \approx 0.02$ .

## VIII. SUMMARY AND DISCUSSIONS

In this paper, we studied the problem of sequential change-point detection when the observations are linear projections of the high-dimensional signals. We were interested in the problem where the change-point causes an *unknown* shift in the mean of the signal, and one would like to detect such a change as quickly as possible. We presented new

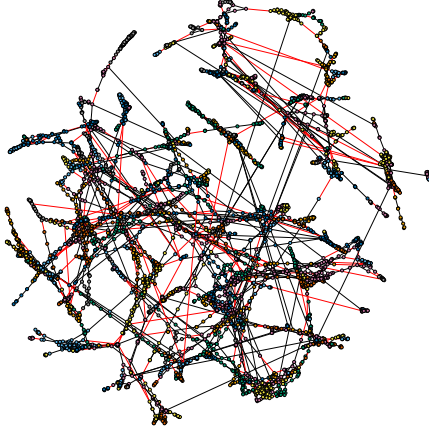


Fig. 11. Power network topology of the Western States Power Grid of the United States.

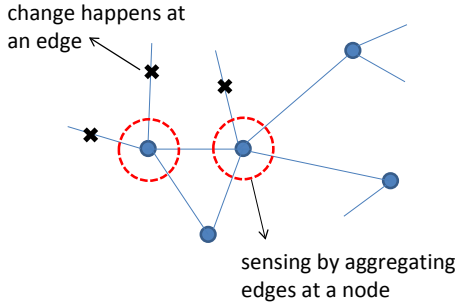


Fig. 12. Illustration of the measurement scheme for a power network. Suppose the physical quantities at edges (e.g., real power flow) at time  $i$  form the vector  $x_i$ , and we can observe the sum of the edge quantities at each node. When there is a power failure, some edges are affected and their means are shifted.

sketching procedures for fixed and time-varying projections, respectively. The sketching procedures were derived based on the generalized likelihood ratio statistic. We analyzed theoretically the performance of our procedures by deriving theoretical approximations to the average run length (ARL) when there is no change, and the expected detection delay (EDD) when there is a change. Our approximations were shown to be highly accurate numerically. We also characterized the performance-complexity trade-off for fixed Gaussian random projection and expander graph projection. We demonstrate the good performance of our procedure using numerical simulations and two real-world examples for solar flare detection and failure detection in power networks.

Thus far, we have assumed that the data streams are independent. In practice, if the data streams are dependent with a *known* covariance matrix  $\Sigma$ , we can whiten the data streams by applying a linear transformation  $\Sigma^{-1/2}x_t$ . Otherwise, the covariance matrix  $\Sigma$  can also be estimated using a training stage via regularized maximum likelihood methods (see [38] for an overview). Alternatively, we may estimate the covariance matrix  $\Sigma'$  of the sketches  $A\Sigma A^T$  or  $A_t\Sigma A_t^T$  directly, which requires fewer samples to estimate due

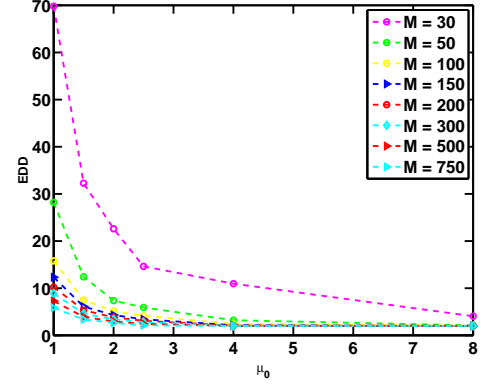


Fig. 13. Power system example:  $A$  being a power network topology constrained sensing matrix. The standard deviation of each point is less than half of the value. EDD versus  $\mu_0$  when we randomly select 5% edges with mean shift  $\mu_0$ .

to the lower dimensionality of the covariance matrix. Then we may build statistical change-point detection procedures using  $\Sigma'$  (similar to what has been done for the projection Hotelling control chart in [9]), which we leave for future work.

#### ACKNOWLEDGEMENT

This work is partially supported by NSF grants CCF-1442635 and CMMI-1538746, and an NSF CAREER Award CCF-1650913.

#### REFERENCES

- [1] Yao Xie, Meng Wang, and Andrew Thompson, "Sketching for sequential change-point detection", in *Global Conference on Signal and Information Processing (GlobalSIP)*, 2015, pp. 78–82.
- [2] A. Tartakovsky, I. Nikiforov, and M. Basseville, *Sequential analysis: Hypothesis Testing and Changepoint Detection*, Chapman and Hall/CRC, 2014.
- [3] H. V. Poor and O. Hadjilaidis, *Quickest detection*, Cambridge University Press, Dec. 2008.
- [4] D. P. Woodruff, "Sketching as a tool for numerical linear algebra", *Foundations and Trends in Theoretical Computer Science*, vol. 10, pp. 1–157, 2014.
- [5] David Siegmund, Benjamin Yakir, and Nancy R Zhang, "Detecting simultaneous variant intervals in aligned sequences", *The Annals of Applied Statistics*, vol. 5, no. 2A, pp. 645–668, 2011.
- [6] G. C. Runger, "Projections and the U-squared multivariate control chart", *J. of Quality Technology*, vol. 28, no. 3, pp. 313–319, 1996.
- [7] O. Bodnar and W. Schmid, "Multivariate control charts based on a projection approach", *Allgemeines Statistisches Archiv*, vol. 89, pp. 75–93, 2005.
- [8] E. Skubalska-Rafajlowicz, "Random projections and Hotelling's  $t^2$  statistics for change detection in high-dimensional data analysis", *Int. J. Appl. Math. Comput. Sci.*, vol. 23, no. 2, pp. 447–461, 2013.
- [9] E. Skubalska-Rafajlowicz, "Change-point detection of the mean vector with fewer observations than the dimension using instantaneous normal random projections", in *Stochastic models, statistics and their applications*, vol. 122. Springer Proc. Math. Stat., 2015.
- [10] D. C. Montgomery, *Introduction to statistical quality control*, Wiley, 2008.
- [11] Mark A Davenport, Petros T Boufounos, Michael B Wakin, and Richard G Baraniuk, "Signal processing with compressive measurements", *Selected Topics in Signal Processing, IEEE Journal of*, vol. 4, no. 2, pp. 445–460, 2010.
- [12] Ery Arias-Castro et al., "Detecting a vector based on linear measurements", *Electronic Journal of Statistics*, vol. 6, pp. 547–558, 2012.
- [13] J. Geng, W. Xu, and L. Lai, "Quickest search over multiple sequences with mixed observations", *arXiv:1302.3826*, Feb. 2013.



- [14] Weiyu Xu and Lifeng Lai, “Compressed hypothesis testing: To mix or not to mix?”, in *Communication, Control, and Computing (Allerton), 2013 51st Annual Allerton Conference on*. IEEE, 2013, pp. 1443–1449.
- [15] George K Atia, “Change detection with compressive measurements”, *Signal Processing Letters, IEEE*, vol. 22, no. 2, pp. 182–186, 2015.
- [16] Zaid Harchaoui, Eric Moulines, and Francis R Bach, “Kernel change-point analysis”, in *Advances in Neural Information Processing Systems*, 2009, pp. 609–616.
- [17] Sylvain Arlot, Alain Celisse, and Zaid Harchaoui, “Kernel change-point detection”, *arXiv preprint arXiv:1202.3878*, 2012.
- [18] Yu Christine Chen, Taposh Banerjee, Alejandro D Domínguez-García, and Venugopal V Veeravalli, “Quickest line outage detection and identification”, *Power Systems, IEEE Transactions on*, vol. 31, no. 1, pp. 749–758, 2016.
- [19] Dmitry Mishin, Kieran Brantner-Magee, Ferenc Czako, and Alexander S Szalay, “Real time change point detection by incremental PCA in large scale sensor data”, in *High Performance Extreme Computing Conference (HPEC), 2014 IEEE*. IEEE, 2014, pp. 1–6.
- [20] F. Tsung and K. Wang, “Adaptive charting techniques: Literature review and extensions”, in *Frontier in Statistical Quality Control*, pp. 19–35. Springer-Verlag, 2010.
- [21] Yuxin Chen, Changho Suh, and Andrea J Goldsmith, “Information recovery from pairwise measurements: A shannon-theoretic approach”, in *Information Theory (ISIT), 2015 IEEE International Symposium on*. IEEE, 2015, pp. 2336–2340.
- [22] Andrew K Massimino and Mark A Davenport, “One-bit matrix completion for pairwise comparison matrices”, in *Proc. Workshop on Signal Processing with Adaptive Sparse Structured Representations (SPARS)*.
- [23] Laura Balzano and Stephen J Wright, “Local convergence of an algorithm for subspace identification from partial data”, *Foundations of Computational Mathematics*, vol. 15, no. 5, pp. 1279–1314, 2015.
- [24] J. E. Jackson, *A user’s guide to principle components*, Wiley, New York, 1991.
- [25] Yao Xie and David Siegmund, “Sequential multi-sensor change-point detection”, *The Annals of Statistics*, vol. 41, no. 2, pp. 670–692, 2013.
- [26] D. Siegmund and E. S. Venkatraman, “Using the generalized likelihood ratio statistic for sequential detection of a change-point”, *Annals of Stat.*, vol. 23, no. 1, pp. 255 – 271, 1995.
- [27] D. Siegmund, *Sequential Analysis: Test and Confidence Intervals*, Springer, Aug. 1985.
- [28] D. Siegmund and B. Yakir, *The statistics of gene mapping*, Springer, 2007.
- [29] Harold Ruben, “The volume of an isotropic random parallelotope”, *Journal of Applied Probability*, vol. 16, no. 1, pp. 84–94, 1979.
- [30] P. Frankl and H. Machara, “Some geometric applications of the beta distribution”, *Ann. Inst. Statist. Math.*, 1990.
- [31] W. Xu and B. Hassibi, “Efficient compressive sensing with deterministic guarantees using expander graphs”, in *Info. Theory Workshop*, 2007.
- [32] D. Burshtein and G. Miller, “Expander graph arguments for message-passing algorithms”, *IEEE Trans. Inf. Theory*, vol. 47, no. 2, pp. 782–790, 2001.
- [33] E. J. Candes, “The restricted isometry property and its implications for compressed sensing”, *Compte Rendus de l’Academie des Sciences, Paris, Serie I*, vol. 342, pp. 589–592, 2008.
- [34] William H Woodall and Matoteng M Ncube, “Multivariate cusum quality-control procedures”, *Technometrics*, vol. 27, no. 3, pp. 285–292, 1985.
- [35] Yao Xie, Jiaji Huang, and Rebecca Willett, “Change-point detection for high-dimensional time series with missing data”, *Selected Topics in Signal Processing, IEEE Journal of*, vol. 7, no. 1, pp. 12–27, 2013.
- [36] Duncan J Watts and Steven H Strogatz, “Collective dynamics of ‘small-world’ networks”, *Nature*, vol. 393, no. 6684, pp. 440–442, 1998.
- [37] A. Abur and A. G. Exposito, *Power system state estimation: Theory and Implementation*, CRC Press, 2004.
- [38] J. Fan, Y. Liao, and H. Liu, “An overview on the estimation of large covariance and precision matrices”, *Econometrics Journal*, , no. 19, pp. C1–C32, 2016.
- [39] M. Abramowitz and I. Stegun, *A handbook of mathematical functions, with formulas, graphs and mathematical tables*, Dover, 10th edition, 1964.
- [40] A. Thompson, *Quantitative analysis of algorithms for compressed signal recovery*, PhD thesis, School of Mathematics, University of Edinburgh, 2012.
- [41] B. Laurent and P. Massart, “Adaptive estimation of a quadratic functional by model selection”, *Ann. Stat.*, vol. 28, no. 5, pp. 1302–1338, 2000.

## APPENDIX

We start by deriving the ARL and EDD for the sketching procedure.

*Proofs for Theorem 1 and Theorem 2.* This analysis demonstrates that the sketching procedure corresponds to the so-called mixture procedure (cf.  $T_2$  in [25]) in a special case of  $p_0 = 1$ ,  $M$  sensors, and the post-change mean vector is  $V^\top \mu$ . In [25], Theorem 1, it was shown that the ARL of the mixture procedure with parameter  $p_0 \in [0, 1]$  and  $M$  sensors is given by

$$\mathbb{E}^\infty\{T\} \sim H(M, \theta_0) / \underbrace{\int_{[2M\gamma(\theta_0)/m_1]^{1/2}}^{[2M\gamma(\theta_0)/m_0]^{1/2}} y \nu^2(y) dy}_{c'(M, b, w)}, \quad (34)$$

where the detection statistic will search within a time window  $m_0 \leq t - k \leq m_1$ . Let  $g(x, p_0) = \log(1 - p_0 + p_0 e^{x^2/2})$ . Then  $\psi(\theta) = \log \mathbb{E}\{e^{\theta g(U, p_0)}\}$  is the log moment generating function (MGF) for  $g(U, p_0)$ ,  $U \sim \mathcal{N}(0, 1)$ ,  $\theta_0$  is the solution to  $\dot{\psi}(\theta) = b/M$ ,

$$H(M, \theta) = \frac{\theta [2\pi \ddot{\psi}(\theta)]^{1/2}}{\gamma(\theta) M^{1/2}} \exp\{M[\theta \dot{\psi}(\theta) - \psi(\theta)]\}, \quad (35)$$

and

$$\gamma(\theta) = \frac{1}{2} \theta^2 \mathbb{E}\{[\dot{g}(U, p_0)]^2 \exp[\theta g(U, p_0) - \psi(\theta)]\}.$$

Note that  $U^2$  is  $\chi_1^2$  distributed, whose MGF is given by  $\mathbb{E}\{e^{\theta U^2}\} = 1/\sqrt{1 - 2\theta}$ . Hence, when  $p_0 = 1$ ,

$$\psi(\theta) = \log \mathbb{E}\{e^{\theta U^2/2}\} = -\frac{1}{2} \log(1 - \theta).$$

The first-order and second-order derivative of the log MGF are given by, respectively,

$$\dot{\psi}(\theta) = \frac{1}{2(1 - \theta)}, \quad \ddot{\psi}(\theta) = \frac{1}{2(1 - \theta)^2} \quad (36)$$

Set  $\dot{\psi}(\theta_0) = b/M$ . We obtain the solution that  $1 - \theta_0 = M/(2b)$ , and  $\theta_0 = 1 - M/(2b)$ . Hence,  $\ddot{\psi}(\theta_0) = 2b^2/M^2$ . We have  $g(x, 1) = x^2/2$ , and  $\dot{g}(x, 1) = x$ .

$$\begin{aligned} \gamma(\theta) &= \frac{\theta^2}{2} \mathbb{E}\{U^2 e^{\frac{\theta U^2}{2}}\} e^{\log \sqrt{1 - \theta}} \\ &= \frac{\theta^2}{2} \cdot \frac{1}{(1 - \theta)^{3/2}} \cdot \sqrt{1 - \theta} = \frac{\theta^2}{2(1 - \theta)}, \end{aligned}$$

where

$$\begin{aligned} \mathbb{E}\{U^2 e^{\frac{\theta U^2}{2}}\} &= \frac{1}{\sqrt{2\pi}} \int x^2 e^{\frac{\theta x^2}{2}} e^{-\frac{x^2}{2}} dx \\ &= \frac{1}{\sqrt{2\pi}} \int x^2 e^{-\frac{x^2}{2(1 - \theta)}} dx = \frac{1}{(1 - \theta)^{3/2}}. \end{aligned}$$

Combining the above, we have that the ARL of the sketching procedure is given by

$$\begin{aligned}\mathbb{E}^\infty\{T\} &= \frac{\theta_0[2\pi \cdot \frac{1}{2(1-\theta_0)^2}]^{1/2}}{c'(M, b, w) \frac{\theta_0^2}{2(1-\theta_0)} \sqrt{M}} e^{\frac{M\theta_0}{2(1-\theta_0)}} (1-\theta_0)^{M/2} + o(1) \\ &= \frac{\sqrt{\pi}}{c'(M, b, w) \theta_0 \sqrt{M}} e^{\frac{M\theta_0}{2(1-\theta_0)}} (1-\theta_0)^{M/2} + o(1).\end{aligned}\quad (37)$$

Next, using the fact that  $1/(1-\theta_0) = 2b/M$ , we have that the two terms in the above expression can be written as

$$\frac{M\theta_0}{2(1-\theta_0)} = \frac{M\theta_0}{2} \frac{2b}{M} = \theta_0 b, \quad (1-\theta_0) = \frac{M}{2b},$$

then (37) becomes

$$\begin{aligned}\mathbb{E}^\infty\{T\} &= \frac{\sqrt{\pi}}{c'(M, b, w) \theta_0 \sqrt{M}} e^{\theta_0 b} \left(\frac{M}{2b}\right)^{\frac{N}{2}} + o(1) \\ &= \frac{2\sqrt{\pi}}{c'(M, b, w) \sqrt{M}} \frac{1}{1 - \frac{M}{2b}} e^{(b - \frac{M}{2})} \left(\frac{N}{2b}\right)^{\frac{N}{2}} + o(1) \\ &= \frac{2\sqrt{\pi}}{c'(M, b, w) \sqrt{M}} \frac{1}{1 - \frac{M}{2b}} \left(\frac{M}{2}\right)^{\frac{M}{2}} b^{-\frac{M}{2}} e^{b - \frac{M}{2}} + o(1).\end{aligned}$$

Finally, note that we can also write

$$\gamma(\theta_0) = \theta_0^2/[2(1-\theta_0)] = (1 - M/(2b))^2/(M/b),$$

and the constant is

$$\begin{aligned}c'(M, b, w) &= \int_{[2M\gamma(\theta_0)/w]^{1/2}}^{[2M\gamma(\theta_0)]^{1/2}} y \nu^2(y) dy \\ &= \int_{\sqrt{\frac{2b}{w}(1 - \frac{M}{2b})}}^{\sqrt{2b(1 - \frac{M}{2b})}} y \nu^2(y) dy.\end{aligned}\quad (38)$$

We are done deriving the ARL. The EDD can be derived by applying Theorem 2 of [25] in the case where  $\Delta = \|V^\top \mu\|$ , the number of sensors is  $M$ , and  $p_0 = 1$ .  $\square$

The following proof is for the Gaussian random matrix  $A$ .

*Proof of Theorem 4.* It follows from (31), and a standard result concerning the distribution function of the beta distribution [39, 26.5.3], that

$$\mathbb{P}\{\Gamma \leq b\} = I_b\left(\frac{M}{2}, \frac{N-M}{2}\right), \quad (39)$$

where  $I$  is the regularized incomplete beta function (RIBF) [39, 6.6.2]. We first prove the lower bound in (33). Assuming  $N \rightarrow \infty$  such that (32) holds, we may combine (39) with [40, Theorem 4.18] to obtain

$$\begin{aligned}\lim_{(M,N) \rightarrow \infty} \frac{1}{N} \ln \mathbb{P}\{\Gamma \leq \delta - \epsilon\} \\ = -\left[\delta \ln\left(\frac{\delta}{\delta - \epsilon}\right) + (1-\delta) \ln\left(\frac{1-\delta}{1-\delta+\epsilon}\right)\right] = -c < 0,\end{aligned}$$

from which it follows that there exists  $\tilde{N}$  such that, for all  $N \geq \tilde{N}$ ,

$$\frac{1}{N} \ln \mathbb{P}\{\Gamma \leq \delta - \epsilon\} < -\frac{c'}{2},$$

which rearranges to give

$$\mathbb{P}\{\Gamma \leq \delta - \epsilon\} < e^{-\frac{c'N}{2}},$$

which proves the lower bound in (33). To prove the upper bound, it follows from (39) and a standard property of the RIBF [39, 6.6.3] that

$$\mathbb{P}\{\Gamma \geq b\} = I_{1-b}\left(\frac{N-M}{2}, \frac{M}{2}\right). \quad (40)$$

Assuming  $N \rightarrow \infty$  such that (32) holds, we may combine (40) with [40, Theorem 4.18] to obtain

$$\begin{aligned}\lim_{(M,N) \rightarrow \infty} \frac{1}{N} \ln \mathbb{P}\{\Gamma \geq \delta + \epsilon\} \\ = -\left[(1-\delta) \ln\left(\frac{1-\delta}{1-\delta-\epsilon}\right) + \delta \ln\left(\frac{\delta}{\delta+\epsilon}\right)\right] = -d < 0,\end{aligned}$$

and the argument now proceeds analogously to that for the lower bound.  $\square$

*Lemma 3.* If a 0-1 matrix  $A$  has constant column sum  $d$ , for every non-negative vector  $x$  such that  $[x]_i \geq 0$ , we have

$$\|Ax\|_2 \geq \sqrt{d}\|x\|_2. \quad (41)$$

*Proof of Lemma 3.* Below,  $A_{ij} = [A]_{ij}$ .

$$\begin{aligned}\|Ax\|_2^2 &= \sum_{i=1}^M \left(\sum_{j=1}^N A_{ij} x_j\right)^2 \\ &\geq \sum_{i=1}^M \sum_{j=1}^N (A_{ij} x_j)^2 = d\|x\|_2^2.\end{aligned}$$

$\square$

*Lemma 4 (Bounding  $\sigma_{\max}(A)$ ).* If  $A$  corresponds to a  $(s, \epsilon)$ -expander with regular degree  $d$  and regular left degree  $c$ , for any nonnegative vector  $x$ ,

$$\frac{\|Ax\|_2}{\|x\|_2} \leq d\sqrt{\frac{N}{M}}, \quad (42)$$

thus,

$$\sigma_{\max}(A) \leq d\sqrt{\frac{N}{M}}. \quad (43)$$

*Proof of Lemma 4.* For any nonnegative vector  $x$ ,

$$\begin{aligned}\|Ax\|_2^2 &= \sum_{i=1}^M \left(\sum_{j=1}^N A_{ij} x_j\right)^2 \\ &= \sum_{i=1}^M \left(\sum_{j=1}^N (A_{ij} x_j)^2 + \sum_{j=1}^N \sum_{l=1, l \neq j}^N (A_{ij} A_{il} x_j x_l)\right) \\ &\leq \sum_{i=1}^M \left(\sum_{j=1}^N (A_{ij} x_j)^2 + \sum_{j=1}^N \sum_{l=1, l \neq j}^N \frac{A_{ij} A_{il}}{2} (x_j^2 + x_l^2)\right)\end{aligned}$$

$$\begin{aligned}
&= \sum_{i=1}^M \sum_{j=1}^N \sum_{l=1}^N \frac{A_{ij} A_{il}}{2} (x_j^2 + x_l^2) \\
&= \sum_{j=1}^N \sum_{l=1}^N \sum_{i=1}^M \frac{A_{ij} A_{il}}{2} (x_j^2 + x_l^2) \\
&\leq \sum_{j=1}^N dc(x_j)^2 \tag{44}
\end{aligned}$$

$$= \frac{d^2 N}{M} \|x\|_2^2. \tag{45}$$

Above, (44) holds since for a given column  $j$ ,  $A_{ij} = 1$  holds for exactly  $d$  rows. And for each row  $i$  of these  $d$  rows,  $A_{il} = 1$  for exactly  $c$  columns with  $l \in \{1, \dots, p\}$ ; (45) holds since  $dN = Mc$ . Finally, from the definition of  $\sigma_{\max}$ , (43) holds.  $\square$

*Proof for Theorem 5.* Note that

$$\begin{aligned}
\Delta &= (\mu^\top V V^\top \mu)^{1/2} = (\mu^\top A^\top U \Sigma^{-2} U^\top A \mu)^{1/2} \\
&\geq \sigma_{\max}^{-1}(A) \|U^\top A \mu\|_2 = \sigma_{\max}^{-1}(A) \|A \mu\|_2, \tag{46}
\end{aligned}$$

where  $\sigma_{\max} = \sigma_{\max}(A)$ , and (46) holds since  $U$  is a unitary matrix. Thus, in order to bound  $\Delta$ , we need to characterize  $\sigma_{\max}$ , as well as  $\|A \mu\|_2$  for a  $s$  sparse vector  $\mu$ . Combining (46) with Lemma 3 and 4, we have that for every nonnegative vector  $\mu$ ,  $[\mu]_i \geq 0$ ,

$$\Delta \geq \frac{1}{d} \sqrt{\frac{M}{N}} \sqrt{d(1-\epsilon)} \|\mu\|_2 = \sqrt{\frac{M(1-\epsilon)}{dN}} \|\mu\|_2. \tag{47}$$

Finally, Lemma 2 characterizes the quantity  $[M(1-\epsilon)/(dN)]^{1/2}$  in (47) and establishes the existence of such an expander graph. When  $A$  corresponds to an  $(\alpha N, \epsilon)$  expander described in Lemma 2,  $\Delta \geq \|\beta \mu\|_2$  for all non-negative signals  $[\mu]_i \geq 0$  for some constant  $\alpha$  and some constant  $\beta = (\rho(1-\epsilon)/d)^{1/2}$ . Done.  $\square$

*Proof for Corollary 1.* We define that  $x \triangleq M/b$ , then Theorem 1 tells us that when  $M$  goes to infinity, we have that

$$\begin{aligned}
\mathbb{E}^\infty\{T\} &= \frac{2\sqrt{\pi}}{c(M, x, w)} \frac{1}{1 - \frac{x}{2}} \frac{1}{\sqrt{M}} \left(\frac{x}{2}\right)^{\frac{M}{2}} \exp\left(\frac{M}{x} - \frac{M}{2}\right) + o(1), \tag{48}
\end{aligned}$$

where

$$c(M, x, w) = \int_{\sqrt{\frac{2M}{xw}}(1-\frac{x}{2})}^{\sqrt{\frac{2M}{x}}(1-\frac{x}{2})} u \nu^2(u) du, \tag{49}$$

and

$$\nu(u) \approx \frac{2/u[\Phi(u/2) - 0.5]}{(u/2)\Phi(u/2) + \phi(u/2)}.$$

Define that  $\gamma \triangleq \mathbb{E}^\infty\{T\}$ . One claim is that when  $M > 24.85$  and  $\gamma \in [e^5, e^{20}]$  there exists one  $x^* \in (0.5, 2)$  such that (48) holds. Next, we prove the claim.

Define the logarithm of the right-hand side of (48) as

follows:

$$\begin{aligned}
p(x) &\triangleq \log(2\sqrt{\pi}) - \log(C(M, x, w)) - \log\left(1 - \frac{x}{2}\right) \\
&\quad + \frac{M}{2} \log \frac{x}{2} + \frac{M}{x} - \frac{M}{2} - \frac{1}{2} \log M.
\end{aligned}$$

Since  $\nu(u) \rightarrow 1$  as  $u \rightarrow 0$  and  $\nu(u) \rightarrow \frac{2}{u^2}$  as  $u \rightarrow \infty$ , we know that  $\int_0^\infty u \nu^2(u) du$  exists. From the numerical integration, we know that  $\int_0^\infty u \nu^2(u) du < 1$ . Therefore,  $-\log(C(M, x, w)) > 0$ . Then,

$$p(0.5) > \left(\frac{3}{2} - \frac{1}{2} \log 4\right) M - \frac{1}{2} \log M + \log(2\sqrt{\pi}) - \log \frac{3}{4}.$$

When  $M > 24.85$ , we have that  $p(0.5) > 20$ . Then, when  $\gamma < e^{20}$  we have that  $p(0.5) - \log \gamma > 0$ .

Next, we prove that we can find some  $x_0 \in (0.5, 2)$  such that  $p(x_0) - \log \gamma < 0$  provided that  $\gamma > e^5$ . Since  $\phi\left(\frac{u}{2}\right) < 0.5$  and

$$0.5 + \frac{1}{\sqrt{2\pi}} \exp\left[-\frac{1}{2} \left(\frac{u}{2}\right)^2\right] \left(\frac{u}{2}\right) \leq \Phi\left(\frac{u}{2}\right) \leq 1,$$

for any  $u > 0$ . We have that

$$\nu(u) > \sqrt{\frac{2}{\pi}} \cdot \frac{\exp\left(-\frac{u^2}{8}\right)}{u+1}.$$

Then, we have that for any  $u > 0$ ,

$$u \nu^2(u) > \frac{2}{\pi} \cdot \frac{u \cdot \exp(-u^2/4)}{(u+1)^2}.$$

We define that  $x_0$  is the solution to the following equation:

$$\sqrt{\frac{2M}{x}} \left(1 - \frac{x}{2}\right) = 1. \tag{50}$$

Then, we have that

$$\begin{aligned}
C(M, x_0, w) &> \frac{2}{\pi} \cdot \int_{1/\sqrt{w}}^1 \frac{u \cdot \exp(-u^2/4)}{(u+1)^2} du \\
&> \frac{2}{\pi} \cdot \int_{1/\sqrt{w}}^1 \frac{u \cdot \exp(-u^2/4)}{4} du \\
&= \frac{1}{\pi} \cdot \left( \exp\left(-\frac{1}{4w}\right) - \exp\left(-\frac{1}{4}\right) \right) \\
&> \frac{1}{\pi} \exp\left(-\frac{1}{4}\right) \cdot \left( \frac{1}{4} - \frac{1}{4w} \right),
\end{aligned}$$

where the second inequality is due to the fact that the upper bound for the integral interval is 1 and the third inequality is due to the fact that  $\exp(-x)$  is a convex function. Therefore, we have that

$$-\log C(M, x_0, w) < \log \pi + \frac{1}{4} - \log\left(\frac{1}{4} - \frac{1}{4w}\right)$$

Note that the upper bound above for  $-\log C(M, x_0, w)$  is not dependent on  $M$ , which is because we choose a  $x_0$  that depends on  $M$ . Solving the equation (50), we have that

$$x_0 = 2 + \frac{1}{M} - \sqrt{\frac{1}{M^2} + \frac{4}{M}} < 2,$$

and  $x_0 \rightarrow 2$  as  $M \rightarrow \infty$ . By Taylor's expansion, we have that  $x_0 = 2 - 2M^{-1/2} + M^{-1} + o(M^{-1})$ , or  $x_0 = 2 - 2M^{-1/2} + o(M^{-1/2})$ . Then, we have that

$$-\log\left(1 - \frac{x_0}{2}\right) = -\log(M^{-1/2}) + o(1),$$

and

$$\begin{aligned} \frac{M}{2} \log \frac{x_0}{2} &= \frac{M}{2} \log(1 - M^{-1/2}) \\ &= \frac{M}{2} \cdot \left(-M^{-1/2} - \frac{1}{2}M^{-1} + o(M^{-1})\right) \\ &= -\frac{1}{2}M^{1/2} - \frac{1}{4} + o(1), \end{aligned}$$

and

$$\begin{aligned} \frac{M}{x_0} &= \frac{M}{2} \cdot \frac{1}{1 - (M^{-1/2} + M^{-1}/2 + o(M^{-1}))} \\ &= \frac{M}{2} \cdot (M^{-1/2} + M^{-1}/2 + o(M^{-1})) \\ &\quad + (M^{-1/2} + M^{-1}/2 + o(M^{-1}))^2 + o(M^{-1}) \\ &= \frac{1}{2}M^{1/2} + \frac{1}{2} + o(1) \end{aligned}$$

Combining the above results, we have that

$$p(x_0) < \log(2\sqrt{\pi}) + \log \pi - \log\left(\frac{1}{4} - \frac{1}{4w}\right) + \frac{1}{2} + o(1). \quad (51)$$

One important observation is that the right-hand side of (51) converges as  $M \rightarrow \infty$ . In fact,  $p(x_0)$  as a function of  $M$  is decreasing and converges as  $M \rightarrow \infty$ . Since we set  $w \geq 100$ , then for any  $M > 24.85$ ,  $p(x_0) < 5$ . Therefore, for any  $\gamma > e^5$  and any  $M > 24.85$ , we can find a  $x_0$  close to 2 such that  $p(x_0) - \log \gamma < 0$ .

Since  $p(x)$  is a continuous function, there exists a solution  $x^* \in (0.5, 2)$  such that equation (48) holds.  $\square$

*Proof of Theorem 3.* By law of large number, when  $t - k$  tends to infinity, the following sum converges in probability

$$\frac{1}{t - k} \sum_{i=k+1}^t \mathbb{I}_{in} \xrightarrow{P} r. \quad (52)$$

Moreover, from central limit theorem,

$$\frac{1}{\sqrt{t - k}} \sum_{i=k+1}^t [x_i]_n (\mathbb{I}_{in} - r) \xrightarrow{d} \mathcal{N}(0, r(1 - r)). \quad (53)$$

So by continuous mapping theorem,

$$\left( \frac{1}{\sqrt{(t - k)r(1 - r)}} \sum_{i=k+1}^t [x_i]_n (\mathbb{I}_{in} - r) \right)^2 \xrightarrow{d} \chi_1^2, \quad (54)$$

i.e., the squared and scaled version of the sum is asymptotically a  $\chi_1^2$  random variable with one degree of freedom. By Slutsky's theorem, combining (52) and (54),

$$\frac{1}{1 - r} \frac{[\sum_{i=k+1}^t [x_i]_n (\mathbb{I}_{in} - r)]^2}{\sum_{i=k+1}^t \mathbb{I}_{in}} \xrightarrow{d} \chi_1^2$$

Using Lemma 1 in [41], for  $X \sim \chi_1^2$ ,

$$\begin{aligned} \mathbb{P}\{X \geq 1 + 2\sqrt{\epsilon} + 2\epsilon\} &\leq e^{-\epsilon} \\ \mathbb{P}\{X \leq 1 - 2\sqrt{\epsilon}\} &\leq e^{-\epsilon} \end{aligned}$$

Therefore, with probability at least  $1 - 2e^{-\epsilon}$ , the difference is bounded by a constant

$$\left( \frac{\sum_{i=k+1}^t [x_i]_n \mathbb{I}_{in}}{\sqrt{\sum_{i=k+1}^t \mathbb{I}_{in}}} - r \frac{\sum_{i=k+1}^t [x_i]_n}{\sqrt{\sum_{i=k+1}^t \mathbb{I}_{in}}} \right)^2 < (1 + 2\sqrt{\epsilon} + 2\epsilon)(1 - r).$$

On the the hand, by central limit theorem, when  $t - k$  tends to infinity,

$$\frac{1}{\sqrt{t - k}} \sum_{i=k+1}^t [x_i]_n \xrightarrow{d} \mathcal{N}(0, 1).$$

and by law of large number and continuous mapping theorem

$$\left( \frac{\sum_{i=k+1}^t \mathbb{I}_{in}}{t - k} \right)^{-1/2} - \frac{1}{\sqrt{r}} \xrightarrow{P} 0$$

Hence, invoking Slutsky's theorem again, we have

$$\left( \frac{\sum_{i=k+1}^t [x_i]_n}{\sqrt{\sum_{i=k+1}^t \mathbb{I}_{in}}} - \frac{\sum_{i=k+1}^t [x_i]_n}{\sqrt{r(t - k)}} \right)^2 \xrightarrow{d} 0$$

Hence, combining the above, by a triangle inequality type of argument, we may conclude that, with high-probability, the difference is bounded by a constant  $c$

$$\left( \frac{\sum_{i=k+1}^t [x_i]_n \mathbb{I}_{in}}{\sqrt{\sum_{i=k+1}^t \mathbb{I}_{in}}} - \sqrt{r} \frac{\sum_{i=k+1}^t [x_i]_n}{\sqrt{(t - k)}} \right)^2 < c.$$

Hence, to control the ARL for  $T_{TV}$  defined in (20)

$$T_{\{0,1\}} =$$

$$\inf\{t : \max_{t-w \leq k < t} \frac{1}{2} \sum_{n=1}^N \frac{\left(\sum_{i=k+1}^t [x_i]_n \mathbb{I}_{in}\right)^2}{\sum_{i=k+1}^t \mathbb{I}_{in}} > b\}, \quad (55)$$

one can approximately consider another procedure

$$\tilde{T}_2 = \inf\{t : \max_{t-w \leq k < t} \frac{1}{2} \sum_{n=1}^N U_{n,k,t}^2 > \frac{b}{r}\},$$

with

$$U_{n,k,t} \triangleq \frac{\sum_{i=k+1}^t [x_i]_n}{\sqrt{t - k}},$$

This corresponds to the special case of the mixture procedure with  $N$  sensors and all being affected by the change ( $p_0 = 1$ ), except that the threshold is scaled by  $1/r$ . Hence, we can use the ARL approximation for mixture procedure, which leads to (25).  $\square$